

# Unharmonised longitudinal data processing using networks

1

June 14, 2019

2

3

## Abstract

4

The main contribution of this work is the use of a simple network representation to allow  
the processing of spatio-temporal demographic data for the identification of data-driven neigh-  
bourhoods and their dynamics, *without the need for geographical harmonisation*, a laborious and  
error-prone process that is currently used in virtually all longitudinal analysis of region-based  
data.

5

6

7

8

9

To allow for a transparent corroboration of our method, we leverage it as basis for an  
interactive and intuitive interface that allows a progressive exploration of the results, from the  
characterisation of broad patterns to the identification of individual details and direct access to  
the original data, including to non-experts.

10

11

12

13

We validate our method with illustrative scenarios for Chicago, Toronto, and Los Angeles,  
with results that match recent literature. The system is publicly available, with data from the  
decennial censuses for over forty regions in the USA and Canada between 1970 and 2010, but  
the methodology is suitable for any region-based data.

14

15

16

17

## 1 Introduction

18

Neighbourhoods have increasingly become a central concept in social research and targets for so-  
cial policy (Sampson, 2012; Galster, 2019; Stone et al., 2015; Looker, 2015). To be sure, a focus  
on neighbourhoods extends to the formative period of the modern social sciences (Abbott, 1997).  
Recent interest has at least partly been rekindled through newly available longitudinal demographic  
datasets (Logan et al., 2014; Manson et al., 2017), convenient computational tools (Rey et al., 2018),  
and new sources of data (Poorthuis, 2018).

19

20

21

22

23

24

25 These advances have made neighbourhood constructs more tractable to quantitative analysis.  
26 Yet new challenges have also emerged, especially at the convergence of research on neighbourhood  
27 effects and neighbourhood dynamics. Neighbourhood effects research assumes knowledge about the  
28 nature and scope of "the neighbourhood" that presumably shapes individual outcomes (Kwan, 2018;  
29 Shelton and Poorthuis, 2019). Concurrently, researchers note that neighbourhoods are not neces-  
30 sarily fixed containers in which other processes occur, but themselves dynamically evolve (Delmelle,  
31 2017; Reades et al., 2019; Li and Xie, 2018). The result is to open up key assumptions about neigh-  
32 bourhoods for theoretical and empirical examination: how do we appropriately define and compare  
33 neighbourhoods at a given time?; how do we appropriately define and compare the temporal tra-  
34 jectories of neighbourhoods?; and can we do both at once, "fully interactionally" (Abbott, 1997):  
35 classify neighbourhoods now based on where they came from and where they are going?

36 In principle, much of the recent research is committed to the proposition that neighbourhoods  
37 are open and evolving entities. Ironically, its empirical practice tends to rely on methods that require  
38 fixed geographical regions. This requirement is difficult to satisfy, as most longitudinal datasets are  
39 based on pre-defined tabulation areas that are routinely modified by data collection agencies, usually  
40 to follow population changes.

41 The standard approach then is to *geographically harmonise* data. This involves interpolating  
42 existing measurements into a common set of regions (Logan et al., 2014; Hallisey et al., 2017;  
43 Allen and Taylor, 2018). Recent computational tools have somewhat simplified this process (Rey  
44 et al., 2018), but it still involves non-trivial questions: which geometry to use as target, how to  
45 apportion the variables, or how to combine data from different sources. Further, these question  
46 do not necessarily have optimal answers. Indeed, regardless of how well this process is performed,  
47 it still introduces errors (Logan et al., 2016), even when additional data is provided (Eicher and  
48 Brewer, 2001). Essentially, harmonisation generates artificial data points that can potentially lead  
49 to inaccurate results, even though they are seldom interpreted as such. Nevertheless, because there  
50 has been no viable alternative, and the results often appear plausible, these concerns are generally  
51 overlooked. The result is that the harmonisation approach is virtually mandatory in the current  
52 literature: "(...) *tract-by-tract comparison is not possible unless data from 2000 is interpolated to*  
53 *2010 boundaries (...)"* (Dmowska et al., 2017), "(...) *This limits cross-year comparison since data*  
54 *are not representative of the same spatial units. (...)"* (Allen and Taylor, 2018).

55 The main contribution of this paper is a method for longitudinal data processing that works with

the original data by leveraging a network based representation. It enables tract-by-tract comparison  
and the identification of patterns of demographic evolution *without geographic harmonisation.*

To allow a proper examination of our method and its results, we built an online interactive  
system using this representation. It enables users to visualise, interpret, and explore trajectories of  
neighbourhood change. This interface helps validate our method, by allowing it to be compared to  
existing and future methods. Further, it is a significant contribution to the research community: it  
provides a vehicle for quickly and easily grasping complex long-term changes, experimenting with  
different parameters to interactively learn from data, and making neighbourhood change research  
publicly transparent. The interface thus responds to increasing concerns about reproducibility and  
transparency, as well as ongoing attention to the value of visualisation in scientific research and  
communication.

We start by presenting an intuitive example of our representation in Section 1, then we review  
the relevant literature on longitudinal studies, data representation, clustering, and spatio-temporal  
visualisation in Section 3. Our methodology is introduced in detail in Section 4, along with the  
included interface. Illustrative scenarios for Chicago, Toronto, and Los Angeles are presented in  
Section 5 and the feedback of five field experts are summarised in Section 6. Our prototype system  
is available at , including more than forty regions in the US and Canada. The source code is publicly  
available at .<sup>1</sup>

## 2 Intuition

While utterly simple, the network model breaks from the deeply rooted traditional tabular paradigm  
in a significant way. Instead of requiring the data as a collection of fixed entities which properties  
evolve over time, literally rows in a table with temporal values as columns, it represents each measure-  
ment as a separate entity and encodes the evolution of these entities over time.

To ease this cognitive transition, we start with an intuitive example of how it works, using a small  
portion of a fictitious urban region illustrated on the left part of Figure 1. This example includes  
three different times ( $t_0, t_1, t_2$ ), with different aggregation areas identified as letters from A to H.  
For  $t_0$ , the initial time, we have areas A and B, with small houses and a park, respectively. The  
park remains stable (B, E, and H), but the houses are partially replaced by larger buildings (C and

---

<sup>1</sup>The editors are considering, at our request, an exception to the double-blind requirement to allow access to the system. We provided them with the URLs of the system, code, and documentation separately.

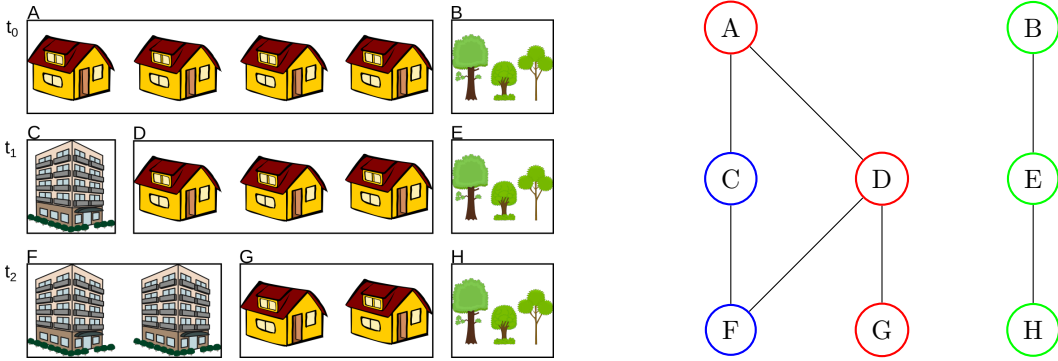


Figure 1: Network based spatio-temporal data representation. **Left:** Three temporal stages of the evolution of a fictitious urban area, with aggregation areas A to H. **Right:** Network representation of the aggregation areas where the colours identify similar regions.

84 F).

85 This example also illustrates some of the challenges of harmonisation. None of these aggregation  
 86 areas is clearly suitable as an interpolation target. In fact, adopting any of these areas as a target  
 87 would require merging heterogeneous regions and/or dividing homogeneous regions. For instance,  
 88 by choosing the regions of  $t_1$ , A would be split to match regions C and D, which appears to be a  
 89 rather reasonable approximation in this homogeneous artificial example, albeit the fallacy of division.  
 90 Region F would be similarly split to match C, but F would be split and merged with G to match  
 91 D, potentially leading to statistical measurements that do not properly represent either region.

92 Real world measurements are seldom as homogeneous and noise-free as this artificial example.  
 93 By splitting and merging the data to fit arbitrary borders, that were not necessarily coherent at the  
 94 time of the measurement, harmonisation increases the distance between measurement and reality.

95 Instead, we propose a network representation. Intuitively, a *network* (also called a *graph*) is  
 96 a collection of entities (nodes) that are related to each other (edges). In this case, each different  
 97 aggregation area is represented as a node and we connect nodes that have overlapping geographical  
 98 areas, leading to the network illustrated on the right of Figure 1. By partitioning the network into  
 99 connected nodes that are similar, we are effectively identifying clusters in the spatio-temporal data,  
 100 as illustrated by the colours of the nodes on the right side of Figure 1. Further, the possible evolution  
 101 paths can also be obtained by computing temporal sequences of nodes, in this case: (A, C, F), (A,  
 102 D, F), (A, D, G), and (B, E, H). This representation is also suited for geographically consistent  
 103 regions, as illustrated by the stable park in this example, and is therefore a generalisation of the

traditional paradigm. 104

Note that the edges of this network merely encode that two regions are related. This is a binary information, there is no apportionment, no areal measurements, no population percentages associated with the edge. Indeed, our method also connects regions of the same time that share borders, representing exactly that they are neighbouring areas. 105  
106  
107  
108

### 3 Related Work 109

Since our problem encompasses several fields, we divide this section into specific sub problems: 110  
111  
112  
113  
114  
*longitudinal demographic studies*, describing the traditional tabular approach to longitudinal studies;   
*data representation*, elaborating how evolving geographic data can be represented for processing; *data clustering*, briefly reviewing existing clustering methods; and *cluster characterisation*, articulating how clusters can be visually summarised.

#### 3.1 Longitudinal demographic studies 115

Census data is used not only to discover demographic patterns (Firebaugh and Farrell, 2016), but to correlate demographic characteristics to other measurements (Diez-Roux et al., 1997). However, longitudinal studies are rare, because they are difficult : ”(...) *One of the most challenging and fascinating areas in spatial statistics is the synthesis of spatial data collected at different spatial scales(...)*” (Gotway and Young, 2002). While census tract level data is readily available for the US since at least 1910 (Manson et al., 2017), most studies consider the period between 1970 and 2010, using pre-harmonised data from the Longitudinal Tract Data Base (Logan et al., 2014). Despite its inherent errors (Logan et al., 2016; Hallisey et al., 2017), this dataset has become the standard source for longitudinal demographic data at the neighbourhood scale, with similar efforts appearing in other countries (Liu et al., 2015; Lee and Rinner, 2015; Allen and Taylor, 2018). These datasets have been highly significant for the field. Yet they also limit the universe of data that can be used to study neighbourhood change, since any new datasets would need to be similarly processed in order to be rendered compatible with these sources. 116  
117  
118  
119  
120  
121  
122  
123  
124  
125  
126  
127  
128

Another option considers the use of grid data (Dmowska et al., 2017; Dmowska and Stepinski, 2018; Stepinski and Dmowska, 2019). Beyond the increased spatial accuracy, this approach does not require complex harmonisation when new data is considered, if the grids are compatible. However, 129  
130  
131

132 demographic data is usually not available in this format, especially from older sources. Additionally,  
133 the conversion from tabulation areas can introduce significant errors.

134 Given these challenges, it is worth considering new alternatives. In this work, we propose a  
135 novel methodology that entirely avoids the problems of geographical harmonisation, considering  
136 each measurement using its actual geographic region. It does not require regions to be consistent  
137 across time because they are naturally represented as different entities.

### 138 3.2 Data representation

139 Network based representation of geographic information is fairly well explored in the literature,  
140 as a basis for topological methods for event detection (Doraiswamy et al., 2014), leveraging signal  
141 processing on graphs (Shuman et al., 2013; Sandryhaila and Moura, 2013) to find patterns and  
142 outliers (Valdivia et al., 2015; Dias and Nonato, 2015; Dal Col et al., 2018). Networks are well  
143 suited to represent trajectories as well (Von Landesberger et al., 2016; Huang et al., 2016; Chen  
144 et al., 2015), allowing the use of graph visualisation methods (Vehlow et al., 2015; Beck et al., 2014).  
145 Our proposed method builds upon this literature. We leverage a network-based representation  
146 that removes the requirement for consistency in the measurement regions. Each region in time  
147 corresponds to a different node. Instead of a collection of time-series, the data is represented as a  
148 dynamic network.

149 Networks have been used to represent census data for clustering purposes (Dias and Nonato,  
150 2015; Setiadi et al., 2017), but these works did not explore temporal evolution, where they are  
151 particularly powerful. Networks allow a natural representation of these inconsistent regions, with  
152 both spatial and temporal connections. There are other possible representations that have similar  
153 properties, but we adopted networks to allow the use of the vast existing literature and methods.

### 154 3.3 Data clustering

155 Data clustering is one of the elementary processes for data analysis, simplifying the data into a  
156 smaller number of homogeneous sets that can be interpreted in the same way. There is no shortage of  
157 contributions for this problem (Fahad et al., 2014), but most neighbourhood related applications still  
158 rely on k-means (Jain, 2010; Delmelle, 2016) and, to a lesser extent, Self Organising Maps (Delmelle,  
159 2017; Ling and Delmelle, 2016).

However, a method for geographic data analysis should not ignore the geographic component of the data, and we extend research exploring ways to incorporate it. One straightforward option for agglomerative methods (Han et al., 2001) is to consider only nearby clusters for merging (Chavent et al., 2017), which can also be done for k-means (Soor et al., 2018). Alternatively, the spatial distance could be directly added to the inter-cluster metric (Chavent et al., 2017) via a mixing parameter, which adds flexibility to the method, but introduces the problem of finding the correct application-dependent values.

Indeed, one crucial step in most clustering algorithms is the definition of the number of clusters. We avoid this problem by considering hierarchical methods (Soille and Najman, 2012), where the result is not a partition of the data, but a tree of partitions, similar to a dendrogram. This approach is interesting for interactive methods, because it allows the user to change the number of clusters on the fly. Since our data is represented as a network, we opted for an heuristic variation of the maximum weighted matching algorithm called *sorted maximal matching* (Dias et al., 2017), which merges clusters based on the weights of the edges between pairs of clusters.

### 3.4 Cluster characterisation

While visualisation has gained prominence as a crucial component of scientific discovery, justification, and communication Tufte et al. (1998), visually representing evolving spatial data is a challenging old problem (Monmonier, 1990; Andrienko et al., 2003; Ferreira, 2015; Zheng et al., 2016).

Most geographic data is naturally bidimensional and maps work well in this case (Zheng et al., 2016; Ward et al., 2015), but the additional temporal dimension cannot be so naturally represented. One straightforward option is to leverage tridimensional plots (Andrienko et al., 2014; Tominski and Schulz, 2012), but this can lead to visual obstructions or scaling problems unless a tridimensional display device is used. A simpler, well adopted, option is to display a map that corresponds to a subset of the temporal information, allowing the user to change the time with an associated control (Chen et al., 2017; Valdivia et al., 2015; Dal Col et al., 2018; Doraiswamy et al., 2014). Small multiples can be used (Von Landesberger et al., 2016), but only when there are few temporal snapshots. However, none of these options is suitable to represent many variables at the same time.

Using data clustering, we can represent the region's cluster instead of all the its variables (Dal Col et al., 2018; Valdivia et al., 2015; Von Landesberger et al., 2016). While this simplifies the geographic portion of the visualization, it introduces the problem of how to summarise the contents of each

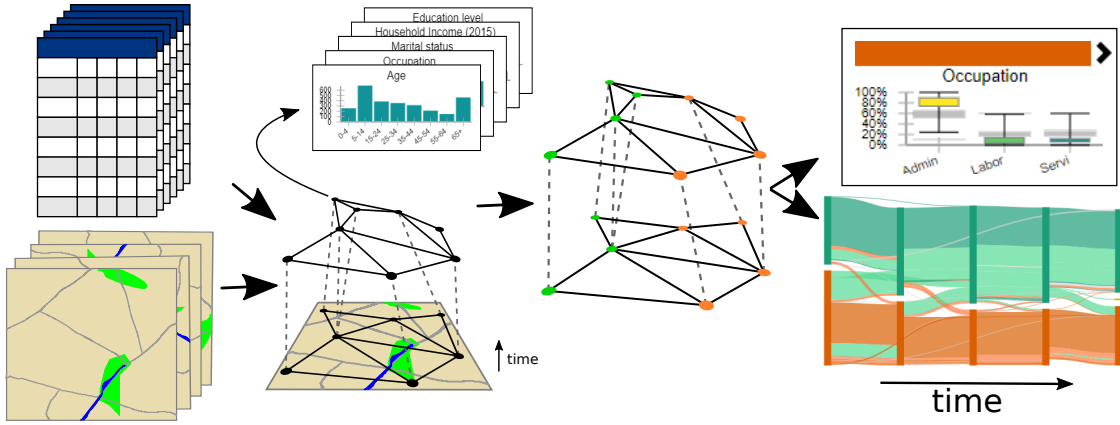


Figure 2: Overview of the proposed method. A network is generated combining the original census data, encoding the changing geographical information. The network is partitioned into an hierarchy (Dias et al., 2017). The characteristics and evolution of the clusters are then visually represented.

cluster. One traditional approach is to use parallel coordinates plot (Ferreira et al., 2015), but these they can get cluttered representing similar clusters over several variables. Further, for demographic applications, the clusters are usually strongly characterised by a small subset of values (Delmelle, 2016, 2017). Therefore, in the proposed method, we identify the variables that are most relevant to the characterisation of each cluster. The distribution of values on that variable is then represented using a boxplot, a well known statistical plot displaying basic properties of the distributions.

## 4 Visualising the demographic spatio-temporal evolution

Figure 2 presents an overview of the processing steps of the proposed method, illustrating how the nodes of the network are used to represent the regions. The following sections elaborate this figure and explain the main features of the interface we built to visualise and explore the evolution of neighbourhoods on the basis of our proposed method.

### 4.1 Census methodology and data representation

Census data is disseminated in a tabulated form for aggregation areas: whole country, state/province, metropolitan region, and so on. To allow for a more meaningful comparison of the data, we aggregated related variables (e.g. White, Black, Asian, Other) into what we called an *aspect* (e.g. Race). The aspects are represented using normalised histograms. This normalisation is crucial for direct

comparison. In essence, it is a generalisation of the standard method of comparing percentages, 206  
since each aggregation area has a different total population. 207

Each area of each census year is represented as a node, and edges are placed between nodes if the 208  
corresponding regions share geographic borders in the same year. Further, edges are placed between 209  
nodes if the corresponding regions belong to sequential years and there is geographical overlap 210  
between them. This approach leads to a single network representing the whole spatio-temporal 211  
space of the data. Our objective then becomes to identify partitions of this network such that the 212  
nodes of each partition are more similar between themselves than to the other nodes. 213

## 4.2 Geographic content clustering 214

Having tied the regions together into a network, we can now partition it to identify similar sets 215  
of regions. We start by adopting a distance function between the nodes, measuring the difference 216  
between the data of the regions. This value is then associated with the edges, leading to a weighted 217  
dynamic network. Every node has a collection of histograms, each representing the distribution of 218  
certain aspect in the population. 219

Let  $G = (V, E)$  be a network, where  $V = \{v_1, v_2, \dots, v_n\}$  is the set of nodes and  $E = \{(v_i, v_j), i \neq 220$   
 $j \text{ and } i, j \in [1, n]\}$  is the set of edges. A function  $H$  associates each node to a set of  $K$  histograms. 221  
We define the distance  $D$  between two nodes  $v_i$  and  $v_j$  as: 222

$$D(v_i, v_j) = \sum_{k \in [1, K]} w_k d(H_k(v_i), H_k(v_j)) \quad (1)$$

where  $d$  is a distance metric between histograms and  $w$  is a sequence of non-negative weights associated 223  
with each aspect,  $\sum_{k \in [1, K]} w_k = 1$ . While any histogram metric can be used, we adopted a 224  
euclidean distance between the vectors, because it led to reasonable results with reduced computational 225  
cost. Therefore the distance between two nodes is defined as the weighted average distance 226  
between its associated histograms, where the weights can be adjusted by the user. 227

Once the distances are associated to the edges, we use watershed cuts (Cousty et al., 2009) to 228  
create an initial clustering, which is then refined into a hierarchy using the Sorted Maximal Matching 229  
(SMM) (Dias et al., 2017) with median linkage. The initial watershed step is performed to create 230  
an initial clustering and reduce the running time of the SMM. We introduced one new parameter to 231  
this method: a maximum distance threshold for the merges, to avoid the early merging of outliers. 232

233 We refer the reader to the original paper (Dias et al., 2017) for more details, including a complete  
234 performance evaluation using several metrics.

235 Each resulting cluster is contiguous in the network. This means that two similar, but non-  
236 contiguous, sets of areas will be classified into two different clusters, which can be counter-intuitive.  
237 To overcome this issue, we *augment* the network with two new edges per node from a nearest  
238 neighbours graph (Pedregosa et al., 2011) using only the distances between the histograms. These  
239 edges connect nodes with similar content, if they are not already connected, providing a path for  
240 the algorithm to group similar nodes.

### 241 4.3 Cluster characterisation and variable relevance

242 A crucial step in understanding neighbourhood change is to characterise the evolving clusters. The  
243 composition of each cluster is represented here by simple statistical measures, considering each aspect  
244 separately. We compute the minimum, maximum, median, 25%, and 75% quantiles for each variable  
245 of each aspect for all clusters in the hierarchy. While interpreting these values is more complex than  
246 interpreting just the average, they provide far more information about the underlying distribution.

247 We also use these statistical measurements to discover what characterises each cluster, that is,  
248 what makes it different from the others. We define the *relevance* of a variable of an aspect based  
249 on the distance between the interquartile ranges (IQR) of the clusters in the same hierarchical  
250 level. If the IQRs overlap for all clusters, that variable is not relevant to the characterisation of the  
251 cluster, but if the IQRs are distant, it means that this specific range of values is something that only  
252 occurs in this cluster. Examining IQRs therefore provides users a straightforward visual method for  
253 determining what variables most clearly define a given cluster.

### 254 4.4 Clusters and trajectories

255 While the partition of the data into different clusters helps the user to understand what groups exist  
256 and where they are, we are also interested in the evolution of these groups. To examine this process  
257 of evolution directly, we introduce the concept of *trajectories*. Trajectories are composed by regions  
258 classified into the same sequence of clusters over the considered period. This enables direct access to  
259 regions that evolved in the same manner. While individual census tracts remain interesting, these  
260 trajectories are the main unit of exploration in this work.

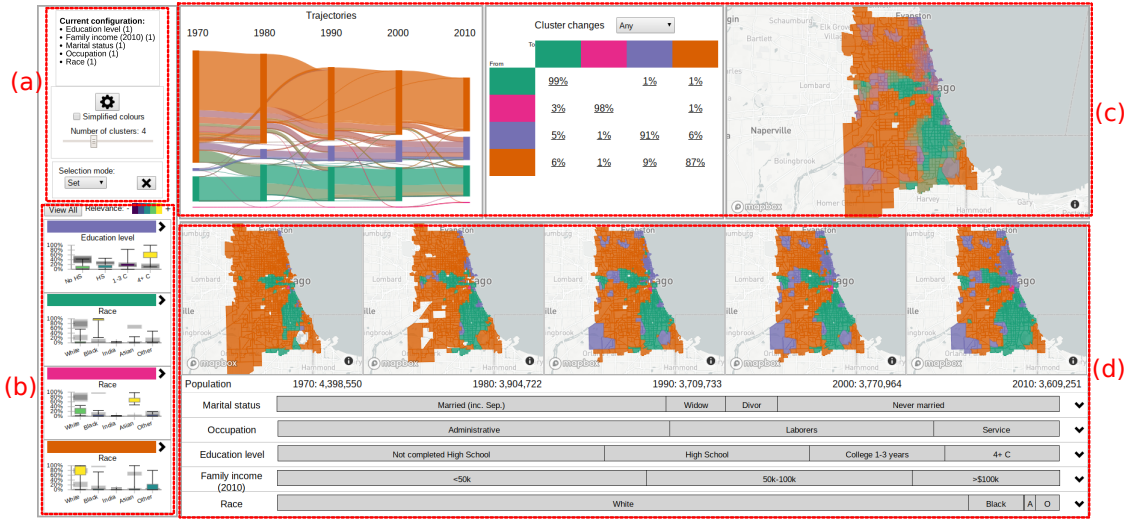


Figure 3: Initial interface of our method showing the demographic evolution of Chicago. **(a)**: Configuration panel with the current clustering parameters and controls. **(b)**: Cluster overview illustrating the most relevant aspect for each cluster. **(c)**: Trajectories overview and the general evolution of the population, geographical information, and how it changed. **(d)**: Details of the selected trajectories, including precise geographic locations, population numbers, and the composition of the aspects.

## 4.5 User interface

To validate and explore the results of our methodology, we built a user interface, illustrated in Figure 3, considering census tract (CT) level data from the Chicago region between 1970 and 2010. This region is known for its entrenched racial divide and the emergence of a '*young urban*' population with a higher education level (Delmelle, 2016, 2017). More details are presented in Section 5.

As illustrated by Figure 3, our proposed interface heavily relies on colour to express cluster-related information. We adopted this convention because colours can be used in all our visual tools in a coherent manner. However, there is a limit on the number of distinct colours that can be used. We limited the number of clusters to eight because this was the largest number of colours that we could reliably and accessibly use, derived from the 8-class Dark2 set from ColorBrewer (Harrower and Brewer, 2003).

The configuration panel, on top left in Figure 3, displays which aspects were used and their weights (following Equation 1). It also includes other configuration options that can be altered without re-processing the data, such as the number of clusters and the colour option. The gear button allows access to the other configuration options that do require further processing, such as changing location, aspects, and weights.

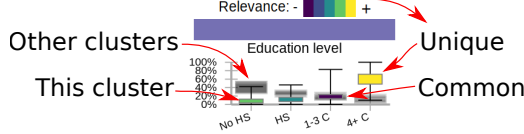


Figure 4: Enhanced boxplot of the clusters’ characteristics allows a quick comparison to the other clusters.

277     The cluster overview panel, on the bottom left in Figure 3, displays a brief summary of each  
 278   cluster, based on the distance between the IQRs, as detailed in Section 4.3. The *View all* button  
 279   opens a new panel where all aspects are included, while the chevron at the side lets the user expand  
 280   each cluster separately.

281     We adopted an *enhanced* version of the traditional boxplot, which includes the IQRs for the other  
 282   clusters, in slightly larger and faded black rectangles. We also colour the current IQR according to  
 283   its relevance. For instance, the boxplot that summarises the purple cluster illustrated in Figure 3,  
 284   detailed on Figure 4, illustrates that this cluster is best defined by the proportion of the population  
 285   with four or more years of college. The user can quickly see that this is relevant because the  
 286   corresponding IQR is coloured with the highest relevance present in the legend. It is also clear  
 287   that, while this cluster includes CTs that have between 10% to 90% of people in this variable,  
 288   approximately, half of them have about 60% of the population with four or more years of college.  
 289   Since all the other IQRs are well separated, this is a defining characteristic of this cluster. Conversely,  
 290   the proportion of the population with one to three years of college is not relevant, as indicated by  
 291   black fill in the rectangle representing the IQR of this cluster, in overlapping position with the  
 292   rectangles of the other clusters. By clicking on the coloured bar above the boxplot, the user can  
 293   select all trajectories that contain this cluster at any point in time.

294     The trajectories overview aims to convey basic information about the trajectories, where they are,  
 295   and what changes are involved. This is done using three sub panels. The first, on the left, contains  
 296   a Sankey diagram illustrating the evolution of the clusters over time. The widths are proportional  
 297   to the population involved. In our example in Figure 3, the orange and green clusters contain most  
 298   of the population and are fairly stable over time. The pink cluster is small and mostly stable. The  
 299   purple cluster is increasing, mostly by incorporating areas that were previously orange. Since the  
 300   purple group corresponds to the emergent ‘young urban’ group, this corroborates the findings of  
 301   Delmelle (Delmelle, 2016, 2017), showing that our network-based method can recover results from

the traditional data processing approach. 302

In the next panel, illustrated in the top middle of Figure 3, is a transition matrix between the 303  
clusters. It indicates a rounded percentage of the population whose area changed between each pair 304  
of clusters. This kind of table can be found in the related literature (Delmelle, 2016), so it is familiar 305  
to the advanced users. It not only informs the proportional changes, but allows the selection of the 306  
corresponding trajectories for further analysis. 307

The panel in the top right of Figure 3 is a map of the region under analysis, summarising the 308  
geographical evolution of the clusters over time. The colours are derived from the clusters involved 309  
in each trajectory, which are consistent across the linked views. 310

The bottom part of the interface contains the details for the selected trajectories, or for the whole 311  
city if nothing is selected, as illustrated in Figure 3. This panel contains two main regions: the small 312  
multiple maps, depicting the clusters at each year, and the stacked bar plots that summarise the 313  
overall composition of these regions. In this example, the maps show the transition from orange to 314  
green and purple in several regions over time. Clicking on a region in these maps will bring up a 315  
new panel with the original census data of this specific region. The actual population numbers are 316  
below the maps. 317

Each aspect is represented by a stacked bar plot, where the width of each rectangle corresponds 318  
to the average percentage of that variable over the considered period. In this case, about half of 319  
the people in Chicago in the considered period are married, and the percentage that are Widowers 320  
or Divorced is roughly similar. About half of the population work in Administrative jobs, a third 321  
never completed high-school, approximately half have gross family income below 50,000USD per 322  
year. The vast majority identify as white. Placing the mouse over one of the bars will open a small 323  
panel with the temporal evolution of that specific variable, and clicking on the chevron on the right 324  
side expands the corresponding aspect, showing details of the temporal evolution of each variable 325  
and also the corresponding IQRs for the whole city. 326

## 5 Illustrative scenarios 327

In this section we present three illustrative scenarios, using decennial census data from the United 328  
States (Manson et al., 2017) and Canada<sup>2</sup>, tabulated by CTs, from 1970 to 2010. The prototype 329

---

<sup>2</sup><http://datacentre.chass.utoronto.ca/census/>

330 interface allows access to 41 regions, 29 in the US and 12 in Canada. New York City was split into  
331 its boroughs to avoid memory crashes on the client browser due to the high number of CTs. We used  
332 five aspects for the USA: Education level, Family income, Marital status, Occupation, and Race;  
333 and seven for Canada: Age, Education level, Home language, Household Income, Marital status,  
334 Occupation, Place of birth, and Religion.

335 While our method does not require geographic harmonisation, it requires matching the variables  
336 over time. The supplementary material contains the details of which census columns were used for  
337 each aspect. Income is slightly inaccurate, even though we did correct for the official inflation. We  
338 grouped the original ranges into three larger ranges, but they do not match precisely.

339 These results are meant to demonstrate the utility of the interface for understanding the evolu-  
340 tionary dynamics of urban neighbourhoods. They also show the face validity of the results generated  
341 by our novel network-based approach.

## 342 5.1 Chicago

343 Our first scenario examines Chicago, focusing on a region loosely following the City's administrative  
344 borders. Its demographic composition is well explored in the literature, with reports of racial divide  
345 and gentrification (Delmelle, 2016, 2017; Hwang and Sampson, 2014), so we expect our results to  
346 contain stable regions where the Race aspect is relevant, and some degree of population change,  
347 with increasing income and education levels.

348 The initial state of the prototype is illustrated in Figure 3. The first step is to identify the  
349 compositions of each cluster from the boxplots, so orange is associated with majority of White  
350 population, green with majority Black, and purple with higher proportion of four years of college  
351 or more (high education level). The expanded version of the boxplots for the purple cluster shows a  
352 higher income level and majority of occupations in administrative jobs, therefore the purple cluster  
353 identifies gentrified regions.

354 The trajectories plot illustrates the process of gentrification, also illustrated in Figure 5, pro-  
355 gressively absorbing regions from the orange cluster (White). This corroborates results from the  
356 literature reporting that Black neighbourhoods are less likely to gentrify (Hwang and Sampson,  
357 2014). Moreover, this process appears to be unidirectional, as indicated by the limited number of  
358 trajectories leaving the purple stream. Next, we select the region that is gentrified in 2010, by click-  
359 ing on the corresponding rectangle in the trajectories plot, updating the information on the maps

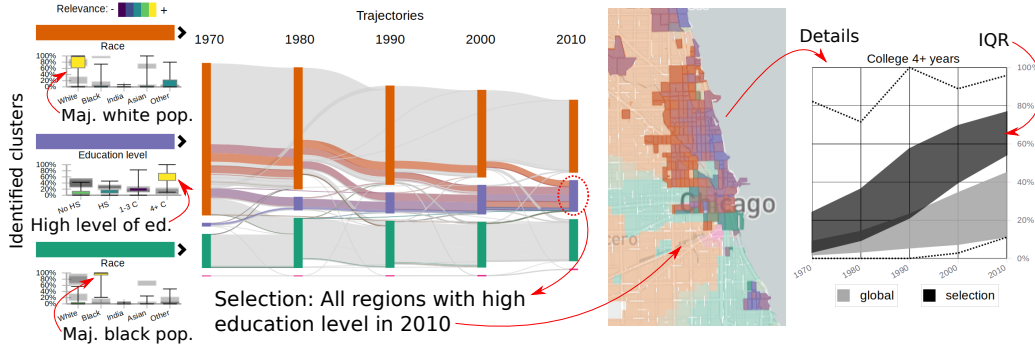


Figure 5: Workflow to discover gentrification in Chicago: the purple cluster corresponds to high education / income. Its population is increasing over time, absorbing from the majority White cluster (orange). By selecting the purple cluster in 2010, the region is highlighted in the maps. The proportion of people with 4+ years of college is increasing in the whole city (grey IQRs), but significantly more in this region (black).

and the details portion of the interface.

The corresponding regions are highlighted in the maps, where the spatial pattern is clear, corresponding exactly to previous findings in the literature based upon harmonisation (Hwang and Sampson, 2014). Further, we can also identify the regions that gentrified earlier on the small maps that depict the involved regions over time. Since the most relevant aspect is Education, specifically "Four or more years of college", we can expand the details of this aspect, as illustrated in the right-most portion of Figure 5, which is increasing for the whole city (grey band), but faster and to a higher level in this region (black band).

## 5.2 Toronto

We consider a region that is approximately the administrative border of the current city of Toronto, using all seven available aspects with equal weights. While Chicago was fairly stable, Toronto is known to be a more dynamic and diverse city, with significant and increasing immigrant population (Hulchanski, 2007). Toronto is also known for a stable and well defined Jewish community (Shahar, 2016). Therefore, we expect the combination of stable and dynamic regions on the results, with Place of Birth, Home Language, and Religion identified as relevant aspects. The results are summarised in Figure 6, considering eight clusters.

The population with low percentage of University degrees is represented in orange, mostly anglophone population in green, Asian immigrants in yellow, high percentage of income in the highest

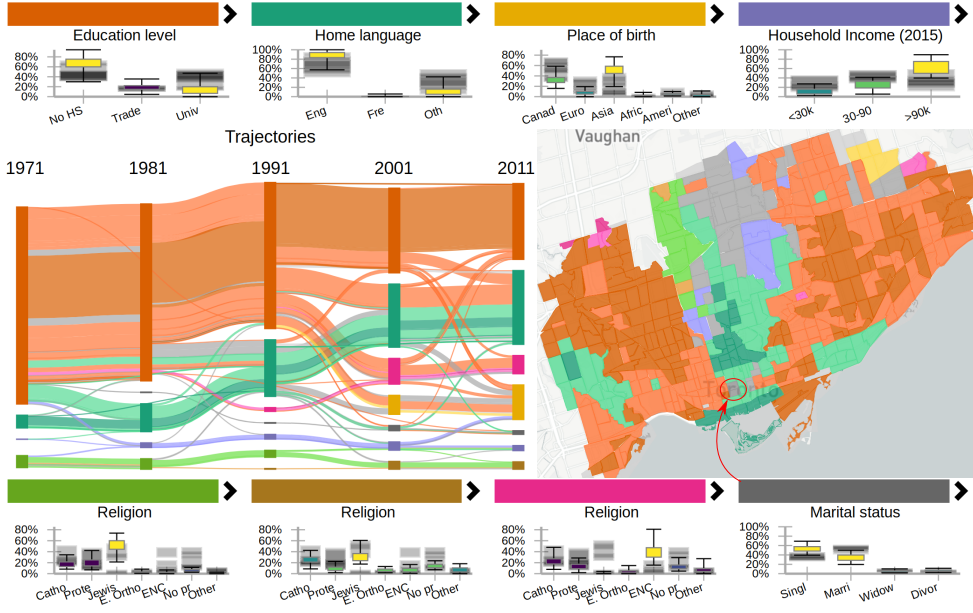


Figure 6: Clustering results for Toronto, with eight clusters, including clusters representing Jewish population, high and low income, low education, and Asian immigration.

378 bracket in purple, high percentage of Jewish people in light green and brown, high percentage of  
 379 Eastern Non-Christian religion in pink, and high concentration of single people in dark grey. From  
 380 the trajectories plot, we can see that Toronto is more dynamic than Chicago, with one cluster con-  
 381 stantly shrinking. In the 1970s, the city was divided into four clusters: low number of university  
 382 degrees, Jewish population, majority anglophones, and high income. Interestingly, the more recent  
 383 clusters that absorbed regions from the orange cluster have similar education profiles and are differ-  
 384 entiated by other aspects. In this sense, the city is growing diverse, changing from a common low  
 385 education profile to a higher level of education with more diversity in religion (pink) and immigration  
 386 (yellow).

387 Indeed, the growing Asian population is visible starting in the 1980s and building thereafter,  
 388 leading to the yellow and pink clusters. While both include a high percentage of people born in  
 389 Asia, the pink is more defined by religion, with low percentage of university degrees, and contains the  
 390 lowest percentage of people in the highest income bracket for these clusters; the yellow is less defined  
 391 by religion, and has higher education and income, geographically corresponding to the Markham  
 392 region, known for its Chinese population. A similar division also happens for the two Jewish clusters,  
 393 where the light green cluster has lower education and income levels than the brown cluster. The  
 394 purple cluster of high income is somewhat stable. Until 2011 the cluster included the Bridle Path

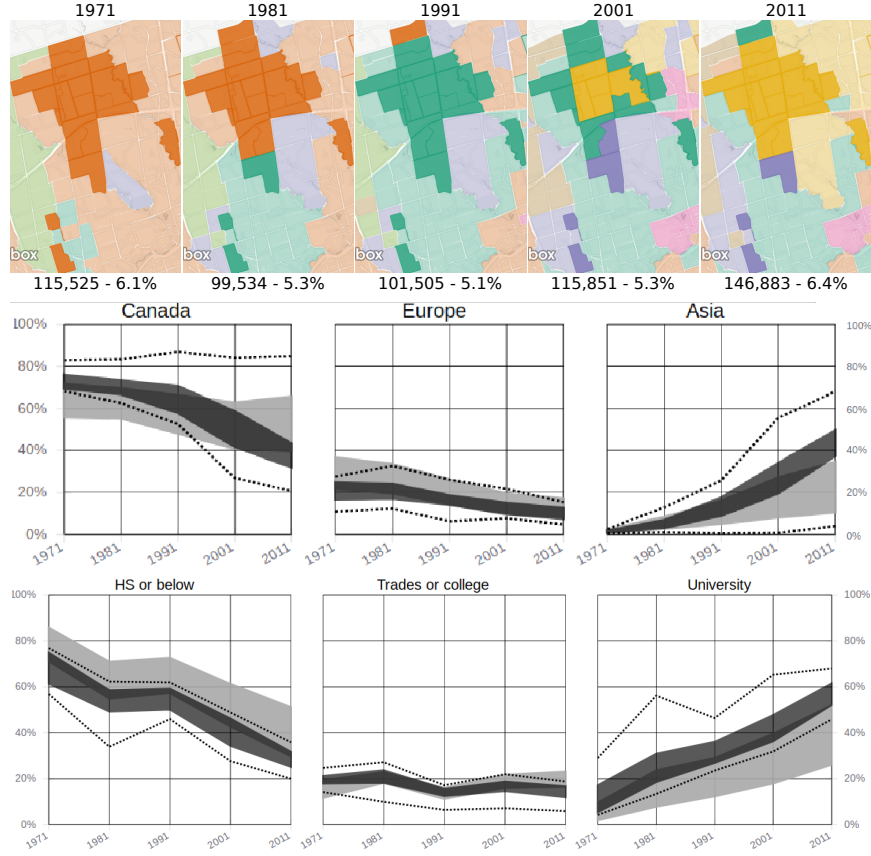


Figure 7: Details for some regions of Toronto that were classified into 3 or more clusters over time.

neighbourhood, known for its wealthy population. In 2011 it was classified into the yellow cluster 395  
of Asian immigration, since about 35% of the population for this CT were then born in Asia. The 396  
income distribution did not change, with 85% of the population with an income of 90k CAD or 397  
more. 398

The most significant indicator of Toronto's dynamism is the presence of grey regions on the map. 399  
These represent regions associated to three or more clusters over this five census period. Using the 400  
'Add' mode for the trajectory selection, we select their trajectories, and a subset of the details is 401  
illustrated in Figure 7. These regions account for about 5% of Toronto's population. The whole 402  
region was classified into the orange cluster in 1971 (low level of university degrees). By 1991, 403  
most of the region was classified into the green cluster, representing anglophone population, mostly 404  
Canadian born, with a higher level of education. As the corresponding plot indicates, this trend in 405  
increasing education is city-wide, but this region has people with better education than most. 406

In 2001, the purple cluster of high income annexes neighbouring parts of the volatile region, and 407

408 the Asian born population increases sharply, as illustrated by the appearance of the yellow cluster.  
409 This cluster indicates well educated, higher income, and about 30%-50% Asian born population. By  
410 2011, the yellow cluster increased considerably, annexing parts of the high income purple cluster,  
411 including the neighbouring Bridle Path area.

412 The geographical borders of the clusters obtained using our method are similar to the regions  
413 presented by previous studies considering Toronto (Hulchanski, 2007), but our interface provides a  
414 deeper insight into their demographic composition, since we consider more data than solely Average  
415 Income, which appears to be a good proxy variable nonetheless. This scenario showcases the ability  
416 of our method and interface to capture and understand the sources of urban volatility.

### 417 5.3 Los Angeles

418 We selected for this scenario a region around the metropolitan area of Los Angeles (LA), following  
419 urban density. While Chicago and Toronto demonstrated the abilities of our method for stable and  
420 dynamic cities, LA is considerably larger, both in population and area. Since our method identifies  
421 only the eight most distinct groups, we expect that some groups not to be identified, especially if  
422 their characterisation is similar to another groups. Further, our system does not include the census  
423 variables related to Hispanic heritage, which were only included in the newer censuses. However,  
424 from the literature, we expect to see some clusters where Race is an important aspect, including  
425 White, Black, and Asian (Reibel, 2003).

426 The summary of the results using all aspects with equal weights and eight clusters is illustrated  
427 in Figure 8. The full statistical description of the clusters is illustrated in Figure 9, where the most  
428 relevant aspect of each cluster is highlighted. From the trajectories plot, we can see that there is a  
429 large but shrinking cluster, depicted in green, one increasing cluster in purple, an almost constant or-  
430 ange cluster, a smaller but increasing pink cluster, and three other small clusters. The corresponding  
431 map illustrates where these clusters are located, and that they are somewhat geographically stable,  
432 with some movement between the green, orange, and purple clusters.

433 From Figure 9, we can see that the green cluster is characterised by a high percentage of White  
434 population, low percentage of population in the lowest income bracket, mostly administrative occu-  
435 pations, and about 30% of the population with four or more years of college. The orange cluster  
436 is characterised by a high percentage of Black population, with few people in the highest range of  
437 income and education. The purple cluster corresponds to a high concentration of "Other" in race,

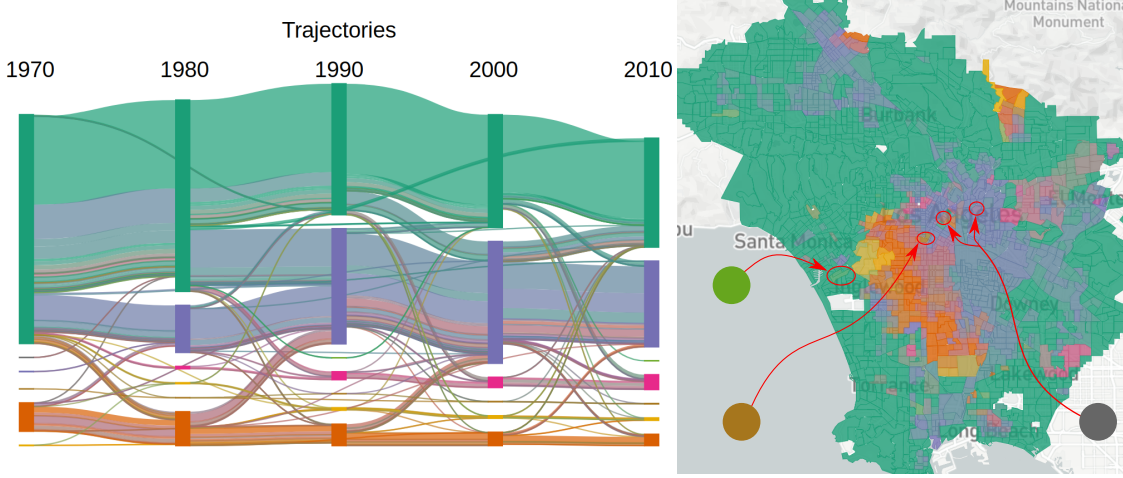


Figure 8: Result for Los Angeles with 8 clusters, including three small and ephemeral clusters. Cluster characterisation is displayed in Figure 9.

which includes Hispanic for this dataset, high concentration of Labourers, and low education and income. The pink cluster contains a high percentage of Asian population and about 30% of the population with four or more years of college. The light green cluster contains very few people in the lower income bracket, mostly White population, with the highest percentage of population with four or more years of college, working administrative jobs, and a high concentration of singles. The yellow cluster represents Black population, with higher level of education and income, mostly working administrative jobs. The brown cluster represent a majority of single population, working administrative jobs with mostly low income. The dark grey cluster is characterised by all its population in the lowest income bracket, low education level, with a majority of White population. Since the extremes in the boxplots of the grey cluster are not significantly different, we can also surmise that this cluster is either small or homogeneous.

The green, orange, and purple clusters present a significant intra-cluster variance in most variables, as indicated by extreme whiskers of the boxplots. While fifty percent of the CTs in the green cluster have between 20% and 40% of people in the lowest income bracket, that cluster also includes CTs where none and all the population belongs to that bracket. This might indicate that this cluster represents different groups of people that are not different enough to be separated at this level of the hierarchy. Conversely, the light green, brown, and dark grey clusters are different enough to be separated into their own clusters at this level, despite being small and ephemeral, including only a few CTs.

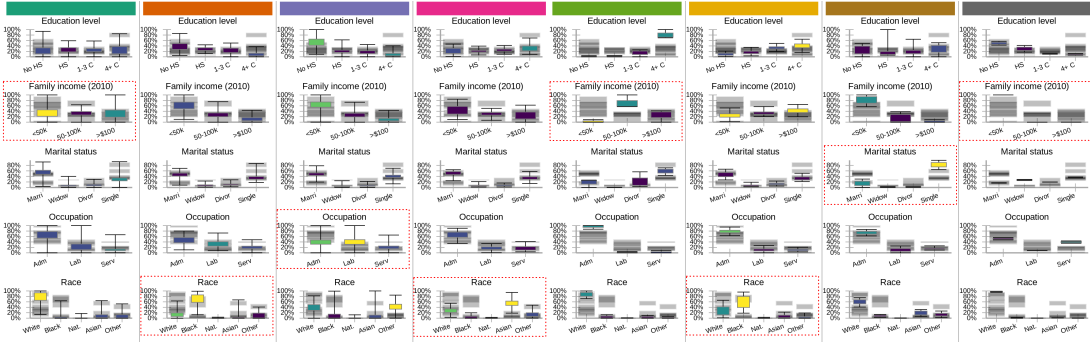


Figure 9: Full characterisation of the eight clusters found for LA. The red rectangles indicate the most relevant aspects for each cluster.

The orange area in the map in Figure 8 presents movement, indicated by the presence of green and purple tones mixed with the orange, which may warrant further exploration. By clicking on the orange bar above the boxplot, we select all trajectories that contain the orange cluster. The corresponding details are illustrated in Figure 10. This shows a location change, where the orange cluster is progressively replaced by the purple cluster on its east side, and in turn expanding to the west. Interestingly, the population increased, the racial profile changed, but the distribution of income was reasonably stable, with a higher amount of the population in the lowest income range and very few people in the highest income range. Indeed, the income difference is significant when compared to the city-wide distribution.

A portion of this region is classified into the green cluster in 2010, indicating a majority white population. To further understand that change, we clear the current selection, and select all regions that changed from orange in 1970 to green in 2010, using the transition matrix. A portion of the resulting region, near the Florence-Graham region, is depicted in Figure 11, along with the temporal evolution of Race. Despite this difference, the other aspects are similar to the ones from the region in Figure 10, with slightly lower income and education profiles. While the racial aspect changed considerably, the economic and educational aspects stayed the same.

These results are visually similar the analysis presented by Dellmelle (Dellmelle, 2016), what was there identified as 'persistently struggling' corresponds to the purple cluster in Figure 8; some portions of the 'stable elite' cluster, near Inglewood, correspond to the high income, high education yellow cluster. The other groups identified by that study were clumped by our system into the green cluster, which would be further divided if more than eight clusters were to be used.

If Toronto illustrates a relatively smooth process of whole-sale diversification, Los Angeles shows

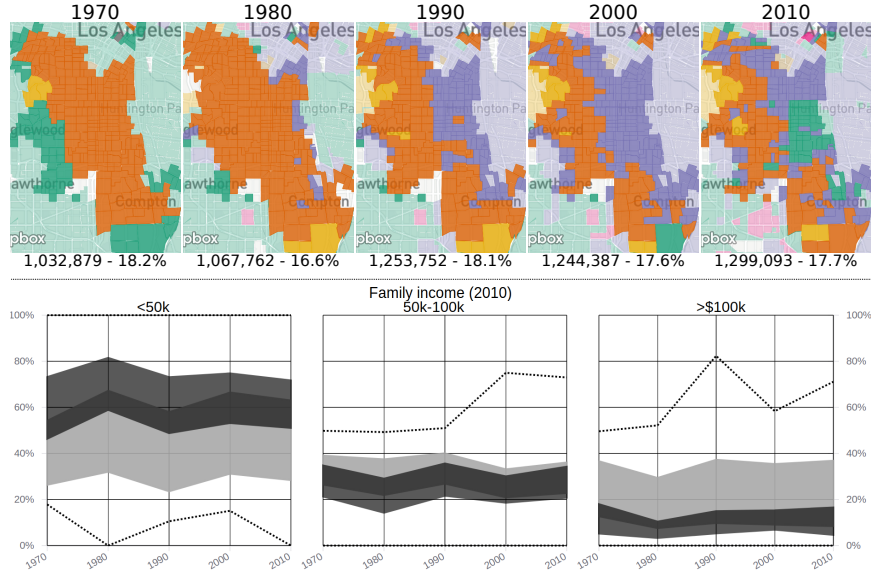


Figure 10: Top: Geographic changes in the majority Black population cluster (orange) and Labourers cluster (green). Bottom: Income evolution for this region (black) and the whole city (grey).

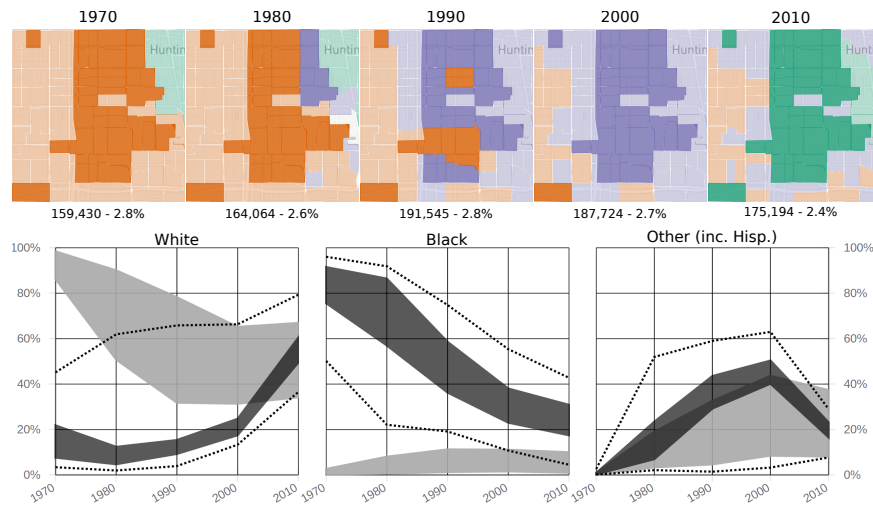


Figure 11: Details for a volatile region contained in the area of Figure 10. This region went from Black to Hispanic to White.

479 the ability of our system and method to uncover more intensive smaller-scale processes of neighbourhood  
480 change. This capacity to examine and classify different types of change operating at different  
481 scales demonstrates the flexibility of the method and tool for advancing the more open-ended notion  
482 of "neighbourhood" envisioned by recent neighbourhood research.

483 While Toronto is more dynamic than Los Angeles, possibly due to size differences, the volatile  
484 regions shown in Figure 7 did not change as quickly or dramatically as the ones shown in Figure 11,  
485 which involved twice as many people. We found this trend to be related to the countries themselves,  
486 Canadian cities have larger areas undergoing slow, gradual changes, whereas American cities have  
487 more general stability, but quicker changes in smaller scales. The supplementary material contains  
488 brief summaries of all the regions accessible in this prototype.

## 489 6 Expert feedback

490 As our method and tool are novel to the field, and somewhat exotic, we subjected them to the  
491 critical scrutiny of experts. We contacted academic and industry experts in sociology and urban  
492 sciences to solicit their evaluation of our methodology. They had access to the prototype tool, a  
493 descriptive documentation of the features (included in the supplementary material), and a sequence  
494 of documentation videos illustrating how to perform specific tasks. The documentation explains  
495 which datasets are used and how the data is represented and processed, noting explicitly that there  
496 is no geographic harmonisation. We focused our inquiries on the results obtained, asking if they  
497 found anything interesting in the data. The message sent and their full response is included in the  
498 supplementary material. Each of the five experts is identified by a letter, from A to E.

499 The overall overall response of the experts was positive, mentioning that the prototype allows  
500 them to analyse census data without the additional work of obtaining and cleaning the data (A, B,  
501 E), and it allows the inclusion of geographic visual analysis tools in their research process (D). It  
502 enables the users to tell different stories about neighbourhoods/cities and their changes (A), visualise  
503 the relationship between key urban variables over time (D), offering a quick way to identify particular  
504 neighbourhoods that one may be interested in studying more in depth around a particular issue or  
505 efficiently understanding the context of an area (E). Indeed, the experts identified gentrification  
506 processes in Manhattan (B) and Dallas (E), reinforced a hypothesis for occupational clustering (D),  
507 and highlighted how the method can be used to compare neighbourhoods and cities (A). In summary,

their view was that the proposed methodology can be a viable alternative for the visual analytics of  
508  
evolving demographic data.  
509

The interface was "easy to navigate" (B), but it was also considered "overwhelming" (A), "in-  
510  
timidating" (E), and "tricky to interpret" (C), possible side-effects of our effort to increase repre-  
511  
sentational accuracy, where we avoided using simplified representation or labels. Identifying clusters  
512  
by their most relevant variables was welcome, but the overlap of information from different clusters  
513  
in the boxplot was "a bit confusing" (C) when colour was not present. Further, most clusters can  
514  
be sufficiently characterised using only the most relevant aspect, but this is not generally true.  
515

While the map of trajectories was mentioned as a "good summary map", how it related to the  
516  
clustering method was unclear (C). The methods include different options on how the colours are  
517  
used, but both are works in progress since reliably representing several distinct entities using colours  
518  
is humanly unfeasible. Indeed, the number of distinguishable colours was a significant constraint,  
519  
we found indications that more clusters should be used in some cases, even if eight clusters is more  
520  
than what is traditionally considered in these analyses. Conversely, increasing the number of clusters  
521  
would also complicate the interpretation of the results.  
522

The experts also mentioned the poor responsiveness of the method when changes in the clustering  
523  
parameters required server-side processing (B,D). Indeed, the current implementation can take a few  
524  
minutes to cluster regions with high number of CTs, like Los Angeles or Brooklyn. Server-processing  
525  
reduced the amount of data transferred to client, but it might increase the response time under load.  
526  
We implemented a cache policy that greatly improved the performance, but fully pre-processing the  
527  
results is not practical due to size of the parameter space.  
528

Most of the experts demonstrated interest in using our method in their research (A, B, D, E),  
529  
aiming to use the census data as a backdrop for other datasets, providing demographic context.  
530  
They also mentioned the need to export subsets of data, plots, and maps to be used in reports and  
531  
publications (C, D, E). More importantly, while these experts were aware that our method does  
532  
not perform geographic harmonisation, none of them mention it. We did not specifically ask if this  
533  
difference led to unexpected results, but rather if they found interesting insights. Most experts found  
534  
phenomena corroborated by the specialised literature, indicating that our methodology produces  
535  
equivalent results, with a fraction of the effort. We interpret the fact that most of them were  
536  
interested in the next steps as confirmation of the accuracy of the method.  
537

538    **7 Discussion and limitations**

539    Our objective was to leverage a network based data representation and visualisation methods for  
540    the exploration of geographically inconsistent region-based data. While we successfully replicated  
541    and corroborated results from the literature, this method still has significant limitations.

542    Removing the need for geographical harmonisation greatly reduces the amount of work necessary  
543    to explore demographic data, but the method still requires consistent variables across the years.  
544    Matching the variables can be trivial for some aspects (Age), but challenging for others (Income).  
545    The divulged income ranges vary over time and the actual values change due to inflation. Some  
546    variables were not considered in earlier censuses, such as Race in Canada, or Hispanic population  
547    in the USA, hampering its use when they are available. Since this is only a prototype, we matched  
548    few aspects, but a proper demographic analysis would benefit from all available information.

549    The limitation on the number of displayed clusters because of the limited number of distinguish-  
550    able colours was significant. While increasing the number of clusters would further complicate an  
551    already complex analysis, it might be warranted for some regions. Colour is a fundamental and  
552    intuitive tool for information representation that can be coherently used across different plots, so  
553    we opted to use it, even if in a limited way. With eight colours, there was overlap between some  
554    clusters, the relevance gradient, and the colour combination.

555    The cognitive load on the user is significant, as we compromised simplicity for accuracy. While  
556    other works labelled the clusters, as 'young urban', 'struggling', and so on (Delmelle, 2016, 2017),  
557    we show the statistical characteristics of the clusters, which are harder to interpret, as the data may  
558    have subtle nuances that labels would otherwise hide. This also led to a crowded interface, mitigated  
559    somewhat the use of pop-up panels and collapsible sections. For some cities, especially if they are  
560    small and stable, the panels can appear redundant, but each provide a different way to interact with  
561    the information that can ease the exploration process for larger and dynamic cities.

562    **8 Conclusion**

563    The objective of this work was to demonstrate that longitudinal studies of evolving regions can  
564    be performed without geographical harmonisation. We proposed an alternative methodology that  
565    robustly considers the data in its original geography, without the creation of arbitrary artificial data  
566    points.

This methodology was then used to create a publicly accessible system, with an interactive and  
intuitive interface, allowing a transparent evaluation and replication of our results. We used this  
interface to corroborate results from the literature and we hope that it will be used to corroborate  
future results as well.

The feedback from experts was positive and most of them were able to extract insight from the  
prototype while indicating interest in using it for their research efforts. Indeed, the experts also  
demonstrated further interest in similar tools, indicating that visual analytics methods that leverage  
user interaction can be valuable in this field. Since our interface can be used by non-experts as well,  
we also contributed to scientific dissemination and stakeholder transparency in urban sciences.

More importantly, we introduced a new idea that, apparently, was never considered in the literature.  
While significant resources were used trying to improve geographical harmonisation, nobody  
questioned if it was really necessary. We proved that it is not necessary, at least for the vast majority  
of demographic studies, especially for neighbourhood effects and neighbourhood dynamics.

## References

- Abbott, A. (1997, 06). Of Time and Space: The Contemporary Relevance of the Chicago School. *Social Forces* 75(4), 1149–1182.
- Allen, J. and Z. Taylor (2018). A new tool for neighbourhood change research: The canadian longitudinal census tract database, 1971–2016. *The Canadian Geographer / Le Géographe canadien*.
- Andrienko, G., N. Andrienko, H. Schumann, and C. Tominski (2014). Visualization of trajectory attributes in space–time cube and trajectory wall. In *Cartography from Pole to Pole*, pp. 157–163. Springer.
- Andrienko, N., G. Andrienko, and P. Gatalsky (2003). Exploratory spatio-temporal visualization: an analytical review. *Journal of Visual Languages & Computing* 14(6), 503–541.
- Beck, F., M. Burch, S. Diehl, and D. Weiskopf (2014). The State of the Art in Visualizing Dynamic Graphs. In R. Borgo, R. Maciejewski, and I. Viola (Eds.), *EuroVis - STARS*. The Eurographics Association.
- Chavent, M., V. Kuentz-Simonet, A. Labenne, and J. Saracco (2017). Clustgeo: an r package for hierarchical clustering with spatial constraints. *Computational Statistics*, 1–24.

- 595 Chen, W., F. Guo, and F.-Y. Wang (2015). A survey of traffic data visualization. *IEEE Transactions*  
596     on Intelligent Transportation Systems 16(6), 2970–2984.
- 597 Chen, W., Z. Huang, F. Wu, M. Zhu, H. Guan, and R. Maciejewski (2017). Vaud: A visual  
598     analysis approach for exploring spatio-temporal urban data. *IEEE Transactions on Visualization*  
599     & Computer Graphics.
- 600 Cousty, J., G. Bertrand, L. Najman, and M. Couprise (2009, Aug). Watershed cuts: Minimum  
601     spanning forests and the drop of water principle. *IEEE Transactions on Pattern Analysis and*  
602     *Machine Intelligence* 31(8), 1362–1374.
- 603 Dal Col, A., P. Valdivia, F. Petronetto, F. Dias, C. T. Silva, and L. G. Nonato (2018). Wavelet-  
604     based visual analysis of dynamic networks. *IEEE Transactions on Visualization and Computer*  
605     *Graphics PP*(99), 1–1.
- 606 Delmelle, E. C. (2016). Mapping the dna of urban neighborhoods: Clustering longitudinal se-  
607     quences of neighborhood socioeconomic change. *Annals of the American Association of Geogra-*  
608     *phers* 106(1), 36–56.
- 609 Delmelle, E. C. (2017). Differentiating pathways of neighborhood change in 50 u.s. metropolitan  
610     areas. *Environment and Planning A: Economy and Space* 49(10), 2402–2424.
- 611 Dias, F. and L. G. Nonato (2015). Some operators from mathematical morphology for the visual  
612     analysis of georeferenced data. In *Workshop on Visual Analytics, Information Visualization and*  
613     *Scientific Visualization - SIBGRAPI*.
- 614 Dias, M. D., M. R. Mansour, F. Dias, F. Petronetto, C. T. Silva, and L. G. Nonato (2017, Oct). A  
615     hierarchical network simplification via non-negative matrix factorization. In *2017 30th SIBGRAPI*  
616     *Conference on Graphics, Patterns and Images (SIBGRAPI)*, pp. 119–126.
- 617 Diez-Roux, A. V., F. J. Nieto, C. Muntaner, H. A. Tyroler, G. W. Comstock, E. Shahar, L. S.  
618     Cooper, R. L. Watson, and M. Szklo (1997). Neighborhood environments and coronary heart  
619     disease: a multilevel analysis. *American journal of epidemiology* 146(1), 48–63.
- 620 Dmowska, A. and T. F. Stepinski (2018). Spatial approach to analyzing dynamics of racial diversity  
621     in large u.s. cities: 1990–2000–2010. *Computers, Environment and Urban Systems* 68, 89 – 96.

Dmowska, A., T. F. Stepinski, and P. Netzel (2017, 03). Comprehensive framework for visualizing and analyzing spatio-temporal dynamics of racial diversity in the entire united states. <i>PLOS ONE</i> 12(3), 1–20.	622 623 624
Doraiswamy, H., N. Ferreira, T. Damoulas, J. Freire, and C. T. Silva (2014, Dec). Using topological analysis to support event-guided exploration in urban data. <i>IEEE Transactions on Visualization and Computer Graphics</i> 20(12), 2634–2643.	625 626 627
Eicher, C. L. and C. A. Brewer (2001). Dasymetric mapping and areal interpolation: Implementation and evaluation. <i>Cartography and Geographic Information Science</i> 28(2), 125–138.	628 629
Fahad, A., N. Alshatri, Z. Tari, A. Alamri, I. Khalil, A. Y. Zomaya, S. Foufou, and A. Bouras (2014, sep). A survey of clustering algorithms for big data: Taxonomy and empirical analysis. <i>IEEE Transactions on Emerging Topics in Computing</i> 2(3), 267–279.	630 631 632
Ferreira, N. (2015). <i>Visual analytics techniques for exploration of spatiotemporal data</i> . Ph. D. thesis, Polytechnic Institute of New York University.	633 634
Ferreira, N., M. Lage, H. Doraiswamy, H. Vo, L. Wilson, H. Werner, M. Park, and C. Silva (2015). Urbane: A 3d framework to support data driven decision making in urban development. In <i>Visual Analytics Science and Technology (VAST), 2015 IEEE Conference on</i> , pp. 97–104. IEEE.	635 636 637
Firebaugh, G. and C. R. Farrell (2016, Feb). Still large, but narrowing: The sizable decline in racial neighborhood inequality in metropolitan america, 1980–2010. <i>Demography</i> 53(1), 139–164.	638 639
Galster, G. C. (2019). <i>Making our neighborhoods, making our selves</i> . University of Chicago Press.	640
Gotway, C. A. and L. J. Young (2002). Combining incompatible spatial data. <i>Journal of the American Statistical Association</i> 97(458), 632–648.	641 642
Hallisey, E., E. Tai, A. Berens, G. Wilt, L. Peipins, B. Lewis, S. Graham, B. Flanagan, and N. B. Lunsford (2017, Aug). Transforming geographic scale: a comparison of combined population and areal weighting to other interpolation methods. <i>International Journal of Health Geographics</i> 16(1), 29.	643 644 645 646
Han, J., M. Kamber, and A. K. Tung (2001). Spatial clustering methods in data mining. <i>Geographic data mining and knowledge discovery</i> , 188–217.	647 648

- 649 Harrower, M. and C. A. Brewer (2003). Colorbrewer.org: An online tool for selecting colour schemes  
650 for maps. *The Cartographic Journal* 40(1), 27–37.
- 651 Huang, X., Y. Zhao, C. Ma, J. Yang, X. Ye, and C. Zhang (2016, Jan). Trajgraph: A graph-based  
652 visual analytics approach to studying urban network centralities using taxi trajectory data. *IEEE*  
653 *Transactions on Visualization and Computer Graphics* 22(1), 160–169.
- 654 Hulchanski, D. J. (2007). The three cities within toronto: Income polarization among toronto's  
655 neighbourhoods, 1970–2005.
- 656 Hwang, J. and R. J. Sampson (2014). Divergent pathways of gentrification: Racial inequality and the  
657 social order of renewal in chicago neighborhoods. *American Sociological Review* 79(4), 726–751.
- 658 Jain, A. K. (2010). Data clustering: 50 years beyond k-means. *Pattern recognition letters* 31(8),  
659 651–666.
- 660 Kwan, M.-P. (2018). The limits of the neighborhood effect: Contextual uncertainties in geographic,  
661 environmental health, and social science research. *Annals of the American Association of Geog-  
662 raphers* 108(6), 1482–1490.
- 663 Lee, A. C.-D. and C. Rinner (2015). Visualizing urban social change with self-organizing maps:  
664 Toronto neighbourhoods, 1996–2006. *Habitat International* 45, 92–98.
- 665 Li, Y. and Y. Xie (2018). A new urban typology model adapting data mining analytics to examine  
666 dominant trajectories of neighborhood change: A case of metro detroit. *Annals of the American  
667 Association of Geographers* 108(5), 1313–1337.
- 668 Ling, C. and E. C. Delmelle (2016). Classifying multidimensional trajectories of neighbourhood  
669 change: a self-organizing map and k-means approach. *Annals of GIS* 22(3), 173–186.
- 670 Liu, X., Y. Song, K. Wu, J. Wang, D. Li, and Y. Long (2015). Understanding urban china with  
671 open data. *Cities* 47, 53 – 61. Current Research on Cities (CRoC).
- 672 Logan, J. R., B. J. Stults, and Z. Xu (2016). Validating population estimates for harmonized census  
673 tract data, 2000–2010. *Annals of the American Association of Geographers* 106(5), 1013–1029.

- Logan, J. R., Z. Xu, and B. J. Stults (2014). Interpolating us decennial census tract data from 674  
as early as 1970 to 2010: A longitudinal tract database. *The Professional Geographer* 66(3),  
412–420. 675  
676
- Looker, B. (2015). *A nation of neighborhoods: imagining cities, communities, and democracy in* 677  
*postwar America*. University of Chicago Press. 678
- Manson, S., J. Schroeder, D. V. Riper, and S. Ruggles (2017). Ipums national historical geographic 679  
information system: Version 12.0 [database]. 680
- Monmonier, M. (1990). Strategies for the visualization of geographic time-series data. *Cartographica:* 681  
*The International Journal for Geographic Information and Geovisualization* 27(1), 30–45. 682
- Pedregosa, F., G. Varoquaux, A. Gramfort, V. Michel, B. Thirion, O. Grisel, M. Blondel, P. Pretten- 683  
hofer, R. Weiss, V. Dubourg, J. Vanderplas, A. Passos, D. Cournapeau, M. Brucher, M. Perrot, 684  
and E. Duchesnay (2011). Scikit-learn: Machine learning in Python. *Journal of Machine Learning* 685  
*Research* 12, 2825–2830. 686
- Poorthuis, A. (2018). How to draw a neighborhood? the potential of big data, regionalization, 687  
and community detection for understanding the heterogeneous nature of urban neighborhoods. 688  
*Geographical Analysis* 50(2), 182–203. 689
- Reades, J., J. D. Souza, and P. Hubbard (2019). Understanding urban gentrification through machine 690  
learning. *Urban Studies* 56(5), 922–942. 691
- Reibel, M. (2003). Measures of geographically uneven subpopulation group change and local group 692  
transitions: Examples from los angeles. *Geographical Analysis* 35(3), 257–271. 693
- Rey, S., E. Knaap, S. Han, L. Wolf, and W. Kang (2018). Spatio-temporal analysis of socioeco- 694  
nomic neighborhoods: The open source longitudinal neighborhood analysis package (oslnap). In 695  
*Proceedings of the 17th Python in Science Conference (SciPy 2018)*, pp. 121–128. 696
- Sampson, R. J. (2012). *Great American city: Chicago and the enduring neighborhood effect*. Uni- 697  
versity of Chicago Press. 698
- Sandryhaila, A. and J. M. Moura (2013). Discrete signal processing on graphs. *IEEE transactions* 699  
*on signal processing* 61(7), 1644–1656. 700

- 701 Setiadi, T., A. Pranolo, M. Aziz, S. Mardiyanto, B. Hendrajaya, and Munir (2017, Oct). A model  
702 of geographic information system using graph clustering methods. In *2017 3rd International*  
703 *Conference on Science in Information Technology (ICSITech)*, pp. 727–731.
- 704 Shahar, C. (2016). *Jewish Population of Canada, 2015*, pp. 261–271. Cham: Springer International  
705 Publishing.
- 706 Shelton, T. and A. Poorthuis (2019). The nature of neighborhoods: Using big data to rethink the  
707 geographies of atlanta’s neighborhood planning unit system. *Annals of the American Association*  
708 *of Geographers* 0(0), 1–21.
- 709 Shuman, D. I., S. K. Narang, P. Frossard, A. Ortega, and P. Vandergheynst (2013). The emerging  
710 field of signal processing on graphs: Extending high-dimensional data analysis to networks and  
711 other irregular domains. *IEEE Signal Processing Magazine* 30(3), 83–98.
- 712 Soille, P. and L. Najman (2012). On morphological hierarchical representations for image processing  
713 and spatial data clustering. In *Applications of Discrete Geometry and Mathematical Morphology*,  
714 pp. 43–67. Springer.
- 715 Soor, S., A. Challa, S. Danda, B. S. Daya Sagar, and L. Najman (2018, July). Extending k-means to  
716 preserve spatial connectivity. In *IGARSS 2018 - 2018 IEEE International Geoscience and Remote*  
717 *Sensing Symposium*, pp. 6959–6962.
- 718 Stepinski, T. F. and A. Dmowska (2019). Imperfect melting pot—analysis of changes in diversity and  
719 segregation of us urban census tracts in the period of 1990–2010. *Computers, Environment and*  
720 *Urban Systems* 76, 101–109.
- 721 Stone, C. N., R. P. Stoker, J. Betancur, S. E. Clarke, M. Dantico, M. Horak, K. Mossberger,  
722 J. Musso, J. M. Sellers, E. Shiao, et al. (2015). *Urban neighborhoods in a new era: Revitalization*  
723 *politics in the postindustrial city*. University of Chicago Press.
- 724 Tominski, C. and H.-J. Schulz (2012). The Great Wall of Space-Time. In M. Goesele, T. Grosch,  
725 H. Theisel, K. Toennies, and B. Preim (Eds.), *Vision, Modeling and Visualization*. The Euro-  
726 graphics Association.
- 727 Tufte, E. R., S. R. McKay, W. Christian, and J. R. Matey (1998). Visual explanations: images and  
728 quantities, evidence and narrative.

- Valdivia, P., F. Dias, F. Petronetto, C. T. Silva, and L. G. Nonato (2015, Oct). Wavelet-based visualization of time-varying data on graphs. In *2015 IEEE Conference on Visual Analytics Science and Technology (VAST)*, pp. 1–8. 729  
730  
731
- Vehlow, C., F. Beck, and D. Weiskopf (2015). The State of the Art in Visualizing Group Structures in Graphs. In R. Borgo, F. Ganovelli, and I. Viola (Eds.), *Eurographics Conference on Visualization (EuroVis) - STARs*. The Eurographics Association. 732  
733  
734
- Von Landesberger, T., F. Brodkorb, P. Roskosch, N. Andrienko, G. Andrienko, and A. Kerren (2016). Mobilitygraphs: Visual analysis of mass mobility dynamics via spatio-temporal graphs and clustering. *IEEE transactions on visualization and computer graphics* 22(1), 11–20. 735  
736  
737
- Ward, M. O., G. Grinstein, and D. Keim (2015). *Interactive data visualization: foundations, techniques, and applications*. AK Peters/CRC Press. 738  
739
- Zheng, Y., W. Wu, Y. Chen, H. Qu, and L. M. Ni (2016, Sept). Visual analytics in urban computing: An overview. *IEEE Transactions on Big Data* 2(3), 276–296. 740  
741